Original Investigation | Özgün Araştırma

Gazi Med J 2026;37(3):436-445

DOI: http://dx.doi.org/10.12996/gmj.2026.4718

Imaging Characteristics and Diagnostic Spectrum of Pancreatic Masses in Pediatric and Young Adult Patients: A Single-Center Retrospective Series

Pediatrik ve Genç Erişkin Hastalarda Pankreatik Kitlelerin Görüntüleme Özellikleri ve Tanısal Spektrumu: Tek Merkezli Retrospektif Bir Seri

Merve Yazol, İsmail Akdulum

Division of Pediatric Radiology, Department of Radiology, Gazi University, Faculty of Medicine, Ankara, Türkiye

ABSTRACT

Objective: We aimed to describe the imaging characteristics and clinicopathologic features of pancreatic masses in pediatric and young adult patients managed at a single tertiary referral center.

Methods: This retrospective study included 19 patients (aged 4–24 years) with a pancreatic mass evaluated between 2012 and 2025. Cross-sectional imaging included computed tomography (n = 12), magnetic resonance imaging (MRI, n = 16), or both (n = 10). Imaging findings, pathologic results, and surgical outcomes were analyzed descriptively.

Results: Solid pseudopapillary neoplasm (SPN) was the most common diagnosis (n = 12, 63.2%), predominantly affecting female patients (10/12, 83.3%), with a median age of 14 years (range 12–17). A well-defined capsule was present in all 12 SPN cases (100%), and internal hemorrhage was present in 58.3%. Two of eleven MRI-evaluated SPN patients demonstrated an atypical, predominantly cystic pattern with absent T1 hyperintensity, no diffusion restriction, and no internal enhancement; both were preoperatively misinterpreted as pseudocysts. Main pancreatic duct dilatation was absent in all SPN cases, regardless of lesion size or location. Surgical resection was performed in 10 of 12 SPN patients (83.3%); lymphovascular invasion was absent in all confirmed cases. Rare entities included pancreatoblastoma (n = 1), diffuse large B-cell lymphoma with pancreatic involvement (n = 1), undifferentiated/anaplastic carcinoma (n = 1; the only case with nodal metastasis in the cohort), neuroendocrine tumor grade 1 (n = 1), focal nesidioblastosis (n = 1), serous cystadenoma (n = 1), and von Hippel-Lindau-associated pancreatic cysts (n = 1).

ÖZ

Amaç: Üçüncü basamak bir referans merkezinde takip edilen pediyatrik ve genç erişkin hastalardaki pankreas kitlelerinin görüntüleme özelliklerini ve klinikopatolojik bulgularını tanımlamayı amaçladık.

Yöntemler: Bu retrospektif çalışmaya, 2012 ile 2025 yılları arasında değerlendirilen ve pankreas kitlesi olan 19 hasta (4–24 yaş arası) dahil edildi. Kesitsel görüntüleme yöntemleri arasında bilgisayarlı tomografi (n = 12), manyetik rezonans görüntüleme (MRG; n = 16) veya her ikisi (n = 10) yer aldı. Görüntüleme bulguları, patoloji sonuçları ve cerrahi sonuçlar tanımlayıcı olarak analiz edildi.

Bulgular: Solid psödopapiller neoplazm (SPN), medyan yaşı 14 (dağılım 12–17) olan ve ağırlıklı olarak kadın hastaları (10/12, %83,3) etkileyen en yaygın tanıydı (n = 12, %63,2). On iki SPN vakasının tamamında (%100) iyi tanımlanmış bir kapsül mevcuttu ve %58,3'ünde iç kanama izlendi. MRG ile değerlendirilen on bir SPN hastasından ikisi, T1 hiperintensitesinin bulunmadığı, difüzyon kısıtlamasının olmadığı ve iç kontrastlanmanın görülmediği, her ikisi de ameliyat öncesi yanlışlıkla psödokist olarak yorumlanan atipik ağırlıklı olarak kistik bir patern sergiledi. Lezyon boyutu veya lokalizasyonundan bağımsız olarak hiçbir SPN vakasında ana pankreatik kanal (MPD) dilatasyonu saptanmadı. SPN hastalarının 12'sinden 10'una (%83,3) cerrahi rezeksiyon uygulandı; doğrulanmış vakaların hiçbirinde lenfovasküler invazyon görülmedi. Nadir görülen antitelere pankreatoblastom (n = 1), pankreas tutulumlu diffüz büyük B hücreli lenfoma (n = 1), andiferansiye/anaplastik karsinom (n = 1; kohortta nodal metastazı olan tek vaka), derece 1 nöroendokrin tümör (n = 1), fokal nezidioblastozis (n = 1), seröz kistadenom (n = 1) ve von Hippel-Lindau ilişkili pankreas kistleri (n = 1) dahildi.

Cite this article as: Yazol M, Akdulum İ. Imaging characteristics and diagnostic spectrum of pancreatic masses in pediatric and young adult patients: a single-center retrospective series. Gazi Med J. 2026;37(3):436-445

Address for Correspondence/Yazışma Adresi: Merve Yazol, Division of Pediatric Radiology, Department of Radiology, Gazi University, Faculty of Medicine, Ankara, Türkiye
E-mail / E-posta: myazol@gmail.com
ORCID ID: orcid.org/0000-0003-1437-8998

Received/Geliş Tarihi: 20.05.2026
Accepted/Kabul Tarihi: 15.06.2026
Publication Date/Yayınlanma Tarihi: 10.07.2026

ABSTRACT

CONCLUSION: SPN accounts for approximately two-thirds of pancreatic masses in pediatric and young adult patients and displays characteristic imaging features that support a confident preoperative diagnosis. An atypical cystic SPN pattern mimicking a pseudocyst on MRI represents an underrecognized diagnostic pitfall. Rare entities have distinct , though sometimes overlapping, imaging appearances, and awareness of the full diagnostic spectrum is important for clinical management in this age group.

Keywords: Solid pseudopapillary neoplasm, pediatric pancreatic mass, pancreatoblastoma, diffuse large B-cell lymphoma, neuroendocrine tumor, MRI

ÖZ

Sonuç: SPN, pediyatrik ve genç erişkin hastalardaki pankreas kitlelerinin yaklaşık üçte ikisini oluşturmaktadır ve güvenilir ameliyat öncesi tanıyı destekleyen karakteristik görüntüleme özellikleri sergiler. MRG'de psödokisti taklit eden atipik kistik SPN paterni, yeterince tanınmayan bir tanısal tuzaktır. Nadir görülen antiteler belirgin ancak zaman zaman birbiriyle örtüşen görüntüleme bulguları taşır ve bu yaş grubundaki klinik yönetim için tüm tanısal yelpazenin farkında olunması önemlidir.

Anahtar Sözcükler: Solid psödopapiller neoplazm, pediyatrik pankreas kitlesi, pankreatoblastom, diffüz büyük B hücreli lenfoma, nöroendokrin tümör, MRG

INTRODUCTION

Pancreatic masses in children and young adults constitute a diagnostically distinct clinical entity compared with those encountered in older adults. The differential diagnosis is dominated by solid pseudopapillary neoplasm (SPN), which accounts for approximately 61% of primary pediatric pancreatic tumors and shows a striking predilection for female patients in the second and third decades of life (1-4).

Pancreatoblastoma is the second most common primary pancreatic tumor in this age group, comprising approximately 17% of cases and representing the most frequent pancreatic malignancy in children below 10 years of age (3). Other exocrine tumors, endocrine tumors, and sarcomas are rare and more commonly encountered in children aged 10 years or older (3). Lymphoma can involve the pancreas primarily or secondarily and represents the most common nonepithelial pancreatic tumor in this age group (5). Although infrequent, pancreatic lymphoma requires a fundamentally different management approach from epithelial tumors and should be recognized as a distinct diagnostic entity (6). At the other end of the spectrum, functional lesions such as focal form of congenital nesidioblastosis may present with no identifiable mass on conventional cross-sectional imaging, rendering the diagnosis dependent on clinical, biochemical, and subtle morphologic correlation (7).

Accurate preoperative characterization of pediatric pancreatic masses directly influences surgical planning, operative approach, and patient counseling. Multimodality imaging integrating ultrasonography (USG), computed tomography (CT), and magnetic resonance imaging (MRI), including diffusion-weighted imaging (DWI) and dynamic contrast enhancement, plays a central role in this process (5). However, imaging features may overlap between entities, and atypical presentations of otherwise characteristic tumors remain an important source of misdiagnosis. Pediatric case series describing the full diagnostic spectrum with detailed imaging-pathology correlation are scarce in the literature, particularly from institutions serving both pediatric and young adult populations (7).

The aim of this study was to describe the imaging characteristics and clinicopathologic features of pancreatic masses in pediatric and young adult patients managed at a single tertiary center, with particular emphasis on the dominant entity, SPN, including its atypical imaging manifestations, and on the salient imaging features of rare diagnoses.

MATERIALS AND METHODS

Study Design and Patients

This was a single-center retrospective study. This study was conducted in accordance with the Declaration of Helsinki. Ethical approval was obtained from the Gazi University Clinical Research Ethics Committee (decision number: 10, date: 02.06.2026). The requirement for informed consent was waived by the ethics commission due to the retrospective design of the study. All patient images included in the manuscript were fully anonymized, and no identifying information is present in the figures. Patients aged 40 years or younger who presented with a pancreatic mass between 2012 and 2025 were eligible. Patients with insufficient imaging, without a confirmed diagnosis, or without active radiologic follow-up were excluded. A total of 19 patients met the inclusion criteria in the final analysis.

Imaging Protocols

Fifteen patients underwent abdominal USG as the primary initial investigation, with Doppler interrogation performed to assess vascularity and vascular contact. CT examinations (available in n = 12 patients) were performed using intravenous iodinated contrast material with a slice thickness of 0.625–1 mm. MRI examinations (available in n = 16 patients)included axial and coronal T2-weighted sequences with and without fat suppression, fat-suppressed T1-weighted sequences before and after intravenous gadolinium contrast administration and DWI with b-value ≥500 s/mm^2. Magnetic resonance cholangiopancreatography was obtained when clinically indicated. Two patients underwent CT only; 10 patients had both CT and MRI; the remainder had multimodality imaging.

Image Analysis

All imaging studies were retrospectively reviewed by a radiologist with 10 years of abdominal imaging experience. The following parameters were recorded: location (head, uncinate process, neck, body, tail, or junction zones), maximum diameter (mm), internal structure (solid, mixed solid-cystic, or predominantly cystic), presence of a capsule or pseudocapsule, internal hemorrhage [T1 hyperintensity on MRI or hyperattenuation on non-contrast CT], calcification, main pancreatic duct (MPD) dilatation, vascular contact or encasement, biliary involvement, enhancement pattern on CT and MRI, and DWI signal characteristics. Distal parenchymal atrophy, when present, was noted.

Statistical Analysis

Continuous variables are expressed as median and interquartile range (IQR); categorical variables are expressed as frequency and percentage (%). Given the descriptive nature and small sample size, no inferential statistical testing was applied. Analyses were performed using SPSS version 22.0 (IBM Corp., Armonk, NY, USA).

RESULTS

Patient Demographics and Clinical Presentation

Nineteen patients (15 females, 4 males; median age 15 years, range 4–24 years) were included. SPN was the most common diagnosis (n = 12, 63.2%), followed by the following rare entities: pancreatoblastoma, diffuse large B-cell lymphoma (DLBCL) with pancreatic involvement, undifferentiated/anaplastic carcinoma, NET G1, focal nesidioblastosis, serous cystadenoma, and von Hippel-Lindau (VHL)-associated pancreatic cysts (n = 1 each). Patient characteristics and imaging modalities are detailed in Table 1.

Among SPN patients, abdominal pain was the predominant complaint (10/12), and symptom duration ranged from acute onset to two years. Two patients were diagnosed incidentally: one following blunt abdominal trauma and one during an obesity workup. A minority of cases exhibited associated symptoms, including nausea, vomiting, and dyspepsia.

Pancreatoblastoma, a rare entity, presented in the patient as a one-year history of intermittent abdominal pain and chronic diarrhea. The DLBCL patient presented with abdominal pain, nausea, and progressive clinical deterioration. The NET G1 patient had nonspecific abdominal pain without biochemical evidence of hormonal excess. The patient with nesidioblastosis presented with recurrent hypoglycemic episodes; biochemical workup confirmed hyperinsulinemic hypoglycemia with inappropriately elevated fasting insulin. The patient with a serous cystadenoma reported subacute abdominal pain without jaundice, weight loss, or steatorrhea. The undifferentiated carcinoma (UC) patient presented with abdominal pain and nausea, without a prior history of pancreatic disease. The VHL patient was asymptomatic, with pancreatic lesions detected on structured surveillance imaging.

Imaging Characteristics

The pancreatic head and uncinate process were the most common sites of involvement, accounting for the largest proportion of SPN lesions (5/12, 41.7%), pancreatoblastoma, and UC of the pancreas. Additional SPN locations included the body-tail (4/12, 33.3%), the body-head junction (2/12, 16.7%), and the neck (1/12, 8.3%); the SPN located in the neck was associated with distal parenchymal atrophy without MPD dilatation. Rare entities were distributed across the pancreatic body (DLBCL), head-body junction (UC of pancreas, NET G1, VHL cysts), uncinate process (serous cystadenoma), and tail (focal nesidioblastosis). The full imaging dataset is provided in Table 2.

Table 1. Demographic and clinical characteristics of all patients (n = 19).

No	Age (y)	Sex	Diagnosis	Presenting symptom	Modality	Surgery
1	12	M	SPN	Abdominal pain (1 month)	USG + CT + MRI	Whipple
2	10	F	SPN†	Abdominal pain	USG + CT + MRI	Refused
3	14	F	SPN	Right upper quadrant pain	USG +CT + MRI	Enucleation
4	18	F	SPN	Incidental (obesity workup)	USG+ MRI	Whipple
5	17	F	SPN	Abdominal pain, vomiting	CT only	Whipple
6	23	F	SPN	Abdominal pain	USG + MRI	Whipple
7	24	F	SPN	Abdominal pain, dyspepsia	USG + MRI	Distal Px
8	16	F	SPN	Abdominal pain, nausea	USG + CT + MRI	Distal Px*
9	12	M	SPN	Abdominal pain (2 years)	USG + CT + MRI	Whipple
10	12	F	SPN	Incidental (post-trauma USG)	USG + CT + MRI	Distal Px
11	12	F	SPN†	Abdominal pain, vomiting	USG + MRI	Refused
12	14	F	SPN	Abdominal pain	CT + MRI	Distal Px
13	15	M	Pancreatoblastoma	Abdominal pain, diarrhea (1 year)	USG + MRI	Enucleation
14	4	F	DLBCL	Abdominal pain, nausea, deterioration	CT only	Core biopsy
15	17	F	UC of pancreas	Abdominal pain, nausea	USG + CT + MRI	Whipple + hepatectomy
16	14	F	NET G1	Abdominal pain	USG + CT + MRI	Whipple
17	15	M	Focal nesidioblastosis	Hyperinsulinemic hypoglycemia	USG + MRI	None
18	21	F	Serous cystadenoma	Abdominal pain, nausea	USG + MRI	Whipple
19	17	M	VHL-associated pancreatic cysts	Incidental (known VHL, surveillance USG)	USG + CT + MRI	None

†Radiologic diagnosis; surgery refused; under follow-up. *Intraoperative perforation; margins not evaluable.
CT: Computed tomography, DLBCL: Diffuse large B-cell lymphoma, MRI: Magnetic resonance imaging, NET: Neuroendocrine tumor, Px: Pancreatectomy, SPN: Solid pseudopapillary neoplasm, UC: Undifferentiated carcinoma, USG: Ultrasonography, VHL: von Hippel-Lindau.

Table 2. Imaging findings for all patients (n = 19).

No	Location	Size (mm)	Structure	Capsule	Hemorrhage	Calcif.	DWI restr.	Enhancement pattern	MPD dil.
1	Head	× 41 × 40	Solid	+	+	–	+	Venous dominant	–
2	Body-head	× 55 × 55	Mixed solid-cystic	+	–	–	+ (periph.)	Peripheral heterogeneous	–
3	Head-uncinate	× 48 × 53	Mixed solid-cystic	+	+	–	N/R	Progressive septal	–
4	Neck	35 × 45	Solid	+	–	–	–	Homogeneous	–
5	Head	60 × 55	Solid	+	+	–	N/A	Heterogeneous	–
6	Uncinate	65 × 60	Hemorrhagic-cystic	+	+	+	–	Peripheral, no solid comp.	–
7	Body-tail	60 × 40	Predominantly cystic	+	–	+	–	No uptake (atypical)	–
8	Head-body	55 × 48	Predominantly cystic	+	–	–	–	No uptake (atypical)	–
9	Head	30 × 27	Mixed solid-cystic	+	–	–	–	Early complete, then wall	–
10	Body-tail	125 × 117	Mixed solid-cystic	+	+	–	+	Peripheral heterogeneous	–
11	Body-tail	26 × 22	Mixed solid-cystic	+	–	–	–	Peripheral solid	–
12	Tail	64 × 63 × 54	Solid-necrotic	+	+	–	N/R	Peripheral heterogeneous	–
13	Head-uncinate	75 × 65	Solid-necrotic	+	+	–	+	Late heterogeneous	Push
14	Body	28 × 22	Solid	–	–	–	N/A	Hypoattenuating	–
15	Head-body	95 × 100 × 115	Solid-necrotic	–	–	–	–	Heterogeneous, necrotic	Biliary
16	Head	51 × 47 × 52	Mixed solid-cystic	+	–	–	–	Mild	–
17	Tail	Hypertrophy	Focal hypertrophy	–	–	–	–	Mildly increased arterial	–
18	Uncinate	27 × 26	Cystic	+	–	–	–	Peripheral only	–
19	Head-body junction	12 × 8 (largest)	Multiple simple cysts (5–6)	–	–	–	–	No internal enhancement	–

Biliary: Biliary dilatation, calcif.: Calcification, comp.: Component, dil.: Dilatation, DWI: Diffusion-weighted imaging, MPD: Main pancreatic duct, MRI: Magnetic resonance imaging, N/A: Not applicable (no MRI), N/R: Not reported, periph.: Peripheral, Push: Ductal displacement without dilatation, restr.: Restriction. Size is given as the maximum dimension on cross-sectional imaging.

Lesion sizes ranged from 12 mm (VHL cysts) to 125 mm (the largest SPN); the median SPN size was 55 mm (IQR 40–61 mm). The UC of the pancreas was the largest among the rare entities (95–115 mm), followed by pancreatoblastoma (75 mm) and NET G1 (51 mm).

In SPNs, a well-defined capsule or pseudocapsule was identified in all 12 cases (100%) and was the most consistent imaging feature. Internal hemorrhage was detected in 7 of 12 patients (58.3%), typically as T1 hyperintensity on MRI. Calcification was present in two cases (16.7%), both of which were peripherally distributed. Mixed solid-cystic morphology was most prevalent (5/12, 41.7%), followed by solid or solid-necrotic morphology (4/12, 33.3%) and predominantly cystic morphology (3/12, 25%). Two of the three predominantly cystic cases demonstrated an atypical pattern (absent T1 hyperintensity, absent diffusion restriction, and absent internal enhancement) and were preoperatively misdiagnosed as either a pseudocyst or a congenital cyst. FNA was attempted in one case but failed to penetrate the thick capsule. DWI restriction was present in 3 of 11 MRI-evaluated patients (27.3%); MPD dilatation was absent in all SPN cases. A representative case is illustrated in Figure 1.

Vascular and ductal involvement was confined to malignant rare entities. The UC of the pancreas encased the portal vein and superior mesenteric vein, produced biliary dilatation by encircling the proximal common bile duct, and extended to fill the portal hilum. Doppler USG showed that the pancreatoblastoma caused ductal displacement without significant dilatation or inferior vena cava (IVC) compression. All SPN cases showed preservation of peripancreatic vascular planes and absence of ductal dilatation, regardless of size and location. Peripancreatic fat planes were preserved in the DLBCL case despite the extent of systemic disease. The NET G1 case demonstrated imaging-pathology size discordance, with a 51 mm mass apparent on imaging harboring a 0.9 cm tumor attributable to desmoplastic stroma.

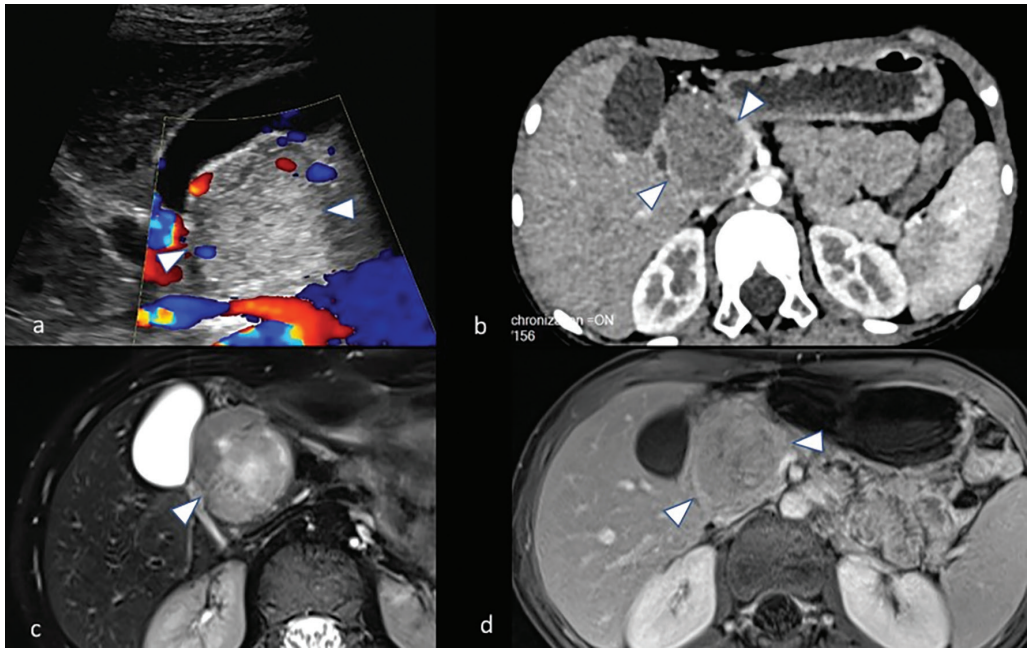

Figure 1. Solid pseudopapillary neoplasm of the pancreatic head in a 12-year-old male. (a) USG demonstrates a 42 × 37 mm well-defined mass with fine internal vascularity on Doppler interrogation. (b) Contrast-enhanced CT shows a heterogeneous solid mass with portal venous phase-dominant enhancement and less than 180° contact with the portal vein confluence and superior mesenteric vein. (c) T2-WI-MRI reveals heterogeneous signal intensity with central cystic foci. (d) Venous-phase contrast-enhanced MRI demonstrates heterogeneous enhancement. Posterior displacement of the inferior vena cava is noted; no peripancreatic lymphadenopathy was identified. Preoperative diagnosis was solid pseudopapillary neoplasm, confirmed on surgical pathology.

Surgical and Pathological Outcomes

Fourteen patients underwent surgical intervention. Pancreaticoduodenectomy was the most frequent operation (n = 8), followed by distal pancreatectomy (n = 4) and enucleation (n = 2). One pancreaticoduodenectomy was combined with hepatectomy in the patient with UC. Four patients were managed non-operatively: two SPN patients refused surgery and remain under imaging surveillance, the nesidioblastosis patient who is under endocrinologic follow-up, and the VHL patient who is on structured surveillance imaging.

Among surgically treated SPN patients (n = 10), histopathology confirmed SPN in all cases; four (40%) were staged as pT3. Surgical margins were negative in 7 of 9 evaluable cases (77.8%); one case could not be assessed due to intraoperative perforation. Two patients had positive anterior margins with uninvolved posterior margins. Perineural invasion (PNI) was identified in three patients (30%); lymphovascular invasion was absent in all ten patients. All dissected lymph nodes were reactive (8–12 nodes per case). Immunohistochemistry demonstrated nuclear and cytoplasmic beta-catenin positivity and chromogranin absence in all confirmed cases (10/10); Ki-67 was 1% in two patients and 5–10% in one patient.

Among rare entities, the pancreatoblastoma was staged as pT3 with negative margins and no perineural or lymphovascular invasion; immunohistochemistry showed nuclear beta-catenin, CK19, pankeratin, synaptophysin, chromogranin, trypsin, and focal AFP positivity. The UC was the only case with lymph node metastasis (pT3pN1, two metastatic nodes); margins were negative, and PNI was present. Immunohistochemistry revealed positivity for vimentin, pankeratin, CK7, and CK20 with negative staining for CD45, chromogranin, AFP, and glypican-3; intracytoplasmic mucin was confirmed by histochemistry. NET G1 pathology confirmed a 0.9-cm grade 1 tumor (Ki-67 1%) that was positive for synaptophysin and chromogranin. Serous cystadenoma was confirmed as a macrocystic/oligocystic type (CK7+, GLUT1+, CAIX+, inhibin+). DLBCL was confirmed on core needle biopsy (CD20+, BCL-2+, Ki-67 90–95%). No resection was performed.

Solid Pseudopapillary Neoplasm

SPN was identified in 12 patients (10 females, 2 males; median age 14 years, IQR 12–17, range 10–24). Ten of 12 patients (83.3%) were symptomatic; abdominal pain was the predominant complaint (10/12, 83.3%). Two patients were diagnosed incidentally: one on post-trauma USG and one on obesity workup USG. Ten patients (83.3%) underwent surgical resection; two refused surgery and remain under radiologic follow-up.

On cross-sectional imaging, SPN most commonly involves the pancreatic head or uncinate process (5/12, 41.7%), followed by body-tail (4/12, 33.3%), body-head junction (2/12, 16.7%), and neck (1/12, 8.3%). The neck lesion was associated with distal parenchymal atrophy without MPD dilatation. The median lesion size was 57 mm (IQR, 40–63; range, 26–125 mm). A well-defined capsule or pseudocapsule was identified in all 12 patients (100%). Internal hemorrhage was detected in 8 of 12 patients (66.7%) across all modalities. Calcification was present in two cases (16.7%), both peripherally distributed. MPD dilatation was absent in all 12 cases.

Internal structure varied across the cohort. Solid morphology was observed in three cases (25%), mixed solid-cystic morphology in 41.7% of cases, and predominantly cystic morphology in three cases (25%).

Two of the three predominantly cystic cases demonstrated an atypical imaging pattern on MRI: no T1 hyperintensity, no diffusion restriction, and no internal enhancement. Both were preoperatively interpreted as pseudocyst or congenital cyst, but surgical pathology confirmed SPN. In one of these cases, FNA was attempted, but it could not penetrate the thick capsule. Central necrosis was identified in two cases (16.7%), both on pathologic examination.

Of 11 patients evaluated with MRI, DWI restriction was present in three (27.3%). Enhancement was predominantly peripheral and heterogeneous in solid and mixed lesions, with venous-phase dominance; the two atypical cases that were predominantly cystic showed no meaningful contrast uptake. On USG, Doppler interrogation demonstrated an absence of significant internal vascularity in most cases.

Among the 10 operated patients, histopathology confirmed SPN in all cases. Surgical procedures included pancreaticoduodenectomy (Whipple; n = 5), distal pancreatectomy (n = 4), and enucleation (n = 1). Intraoperative perforation occurred in one case, precluding margin assessment. Surgical margins were negative in 7 of the remaining 9 cases (77.8%); two patients had positive anterior margins but uninvolved posterior margins. PNI was identified in three of the ten confirmed cases (30%) and lymphovascular invasion was absent in all ten confirmed cases. Four operated cases (40%) were staged as pT3. All dissected lymph nodes were reactive (range: 8–12 nodes per case). Immunohistochemistry revealed nuclear and cytoplasmic beta-catenin positivity and absence of chromogranin in all confirmed cases. Ki-67 was 1% in two patients and 5–10% in one. Imaging findings and pathologic data are summarized in Tables 2 and 3.

Table 3. Imaging and pathologic features of the SPN subgroup (n = 12).

Feature	Value	Notes
Sex (female)	10/12 (83.3%)	males: patients 1, 9
Median age, years (IQR)	(12–17)	Range 10–24
Pathologic confirmation	10/12 (83.3%)	refused surgery (pts 2, 11)
Symptomatic presentation	10/12 (83.3%)	2 incidentals: post-trauma USG, obesity workup
Location: head/uncinate	5/12 (41.7%)	Pts 1, 3, 5, 6, 9
Location: body-head junction	2/12 (16.7%)	Pts 2, 8
Location: neck	1/12 (8.3%)	Pt 4; with distal parenchymal atrophy
Location: body-tail	4/12 (33.3%)	Pts 7, 10, 11, 12
Median size, mm (IQR)	57 (41–64)	Range 26–125
Structure: solid/solid-necrotic	4/12 (33.3%)	Pts 1, 4, 5, 12
Structure: mixed solid-cystic	5/12 (41.7%)	Pts 2, 3, 9, 10, 11
Structure: predominantly cystic	3/12 (25%)	Pts 6, 7, 8 — 2 misdiagnosed as pseudocyst
Capsule present	12/12 (100%)	Present in all cases
Hemorrhage (imaging/pathology)	7/12 (58.3%)	Pts 1, 3, 5, 6, 10, 12; incl. pathologic hemorrhagic spaces
Calcification	2/12 (16.7%)	Pts 6, 7; peripherally distributed
MPD dilatation	0/12 (0%)	Absent in all
DWI restriction (MRI cases)	3/11 (27.3%)	11 SPN patients had MRI; pt 5 CT only
Atypical MRI (pseudocyst pattern)	2/11 (18.2%)	Pts 7, 8: no T1 signal, no DWI, no uptake
Central necrosis on pathology	2/10 (20%)	Pts 10, 12
Surgical resection	10/12 (83.3%)	2 refused surgery (pts 2, 11)
Whipple (pancreaticoduodenectomy)	5/10 (50%)	Head/uncinate lesions (pts 1, 4, 5, 6, 9)
Distal pancreatectomy	4/10 (40%)	Body-tail lesions (pts 7, 8, 10, 12)
Enucleation	1/10 (10%)	Pt 3
Negative surgical margins	7/9 (77.8%)	1 not evaluable (perforation, pt 8)
Positive anterior margin	2/9 (22.2%)	Pts 1, 9; posterior margins uninvolved
PNI	3/10 (30%)	Pts 1, 4, 9
LVI	0/10 (0%)	Absent in all operated cases
Lymph node metastasis	0/10 (0%)	All reactive
pT3 staging	4/10 (40%)	Peripancreatic fat or adjacent organ invasion
Beta-catenin nuclear + (IHC)	10/10 (100%)	All confirmed cases
Chromogranin – (IHC)	10/10 (100%)	Negative in all

*Intraoperative perforation; margins not evaluable. Atypical pseudocyst pattern: Two cases with no T1 hyperintensity, no DWI restriction, and no internal enhancement.

CT: Computed tomography, DWI: Diffusion-weighted imaging, IHC: Immunohistochemistry, IQR: Interquartile range, LVI: Lymphovascular invasion, MPD: Main pancreatic duct, MRI: Magnetic resonance imaging, PNI: Perineural invasion, pt/pts: Patient/patients, Px: Pancreatectomy, SPN: Solid pseudopapillary neoplasm, T1: T1-weighted imaging, USG: Ultrasonography.

Rare Entities: Case Descriptions

Pancreatoblastoma was confirmed in a 15-year-old male presenting with a one-year history of abdominal pain and diarrhea. USG demonstrated a 61 × 51 mm solid, lobulated pancreatic head mass with internal vascularity and IVC compression on Doppler. MRI confirmed a 65 × 75 mm mass involving the head and uncinate process, exhibiting internal microcystic foci, focal necrosis, and late-phase heterogeneous enhancement with associated ductal displacement. Total excision was performed; pathology revealed pancreatoblastoma (pT3, 8 cm) with squamoid nests, negative margins, and absent PNI and LVI. Imaging findings are illustrated in Figure 2.

DLBCL with pancreatic involvement was identified in a 4-year-old female who presented with abdominal pain, nausea, and clinical deterioration. CT demonstrated a 28 × 22 mm hypoattenuating mass in the pancreatic body, with multisegmental colonic wall thickening and diffuse ascites. Core needle biopsy confirmed high-grade B-cell lymphoma (Ki-67 90–95%); chemotherapy was initiated without surgical resection. Undifferentiated (anaplastic) carcinoma was identified in a 17-year-old female patient presenting with abdominal pain and nausea. CT and MRI revealed a 95–115 mm mass encasing the portal vein and the superior mesenteric vein, with biliary dilatation and cystic-necrotic areas. A Whipple procedure with hepatectomy yielded a 7-cm undifferentiated carcinoma (pT3pN1) with positive PNI and two metastatic peripancreatic lymph nodes (the only nodal metastases in the cohort). A diagnosis of NET G1 was confirmed in a 14-year-old female patient presenting with nonspecific abdominal pain. All three modalities demonstrated a 47–51 mm encapsulated mixed solid-cystic head mass; Whipple pathology confirmed a 0.9 cm grade 1 tumor surrounded by desmoplastic stroma, which accounted for the mass size apparent on imaging. Focal nesidioblastosis was suspected in a 15-year-old male with recurrent hyperinsulinemic hypoglycemia. MRI demonstrated focal tail hypertrophy with a lobulated contour, mildly elevated T1 signal, and slightly increased arterial enhancement without DWI restriction. No surgery was performed.

Serous cystadenoma was confirmed histologically in a 21-year-old woman with subacute abdominal pain. MRI demonstrated a 27 × 26 mm unilocular cystic uncinate lesion with peripheral enhancement and an absent solid component; pathology confirmed a macrocystic/oligocystic serous cystadenoma (CK7, GLUT1, CAIX, inhibin+). VHL-associated pancreatic cysts were identified in a 17-year-old male during structured surveillance. USG, CT, and MRI demonstrated 5–6 simple cysts, the largest measuring 12 × 8 mm, without solid components or MPD communication; no intervention was performed.

DISCUSSION

This single-center retrospective series of 19 pediatric and young adult patients demonstrates that SPN is the dominant entity, accounting for approximately two-thirds of cases, consistent with data from large multicenter registries (3,8). The remaining patients harbored a spectrum of diagnostically challenging lesions, including malignant tumors, functional disorders, syndromic cysts, and benign neoplasms, each with distinct but at times overlapping imaging features that directly influenced clinical management (8).

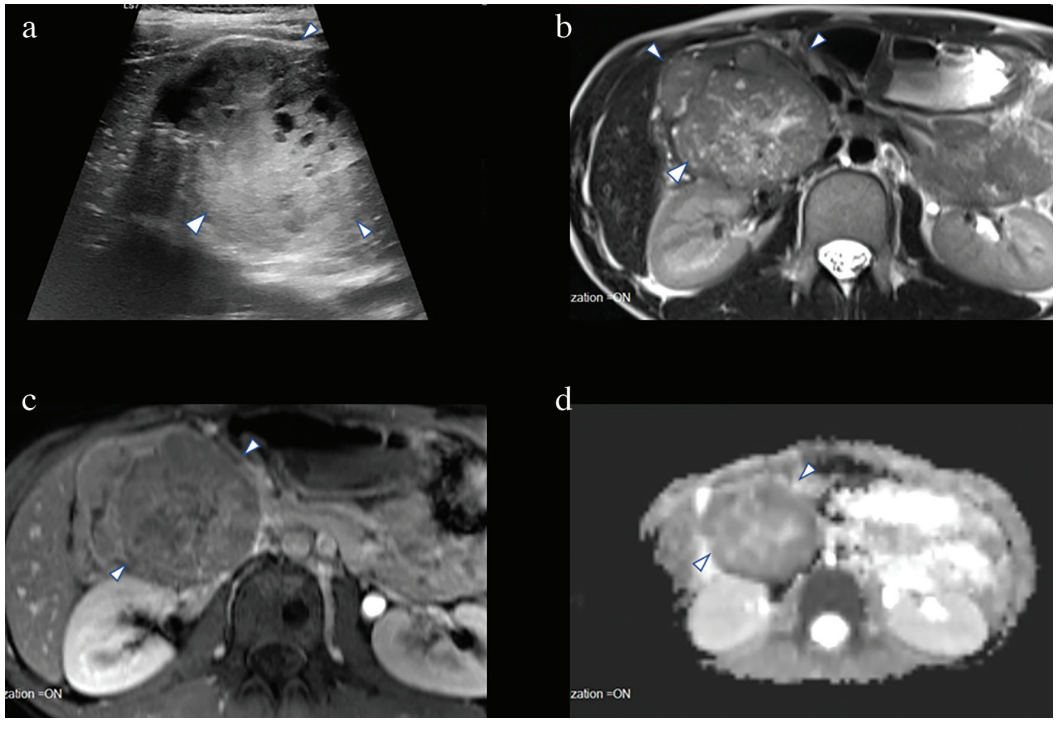

Figure 2. Pancreatoblastoma of the pancreatic head-uncinate process in a 15-year-old male. (a) USG demonstrates a 61 × 51 mm well-defined solid mass with lobulated superior-lateral contour, millimetric internal cysts, and inferior vena cava compression. (b) T2-WI-MRI reveals a large head-uncinate mass with internal microcystic foci and focal necrosis. (c) Late-phase contrast-enhanced MRI demonstrates heterogeneous enhancement. (d) DWI shows diffusion restriction within the lesion.

SPN represents approximately 1–3% of all exocrine pancreatic tumors and nearly 9% of cystic pancreatic neoplasms, with a marked predilection for young females; pooled analyses report female proportions of 84–88% and a mean age at diagnosis of 28–29 years (1,9). In the present cohort, 83.3% of patients were female, with a median age of 14 years; this is consistent with previously reported pediatric and young-adult series and likely reflects both earlier disease manifestation and referral patterns to tertiary pediatric centers. Abdominal pain was the predominant presenting symptom (83.3%), consistent with prior reports in which abdominal pain or discomfort was identified in 63.6% of patients as the most frequent complaint, though 38.1% were asymptomatic at diagnosis, while less frequent presentations included palpable mass, nausea, vomiting, and weight loss, with pancreatitis and jaundice occurring rarely (9). In our series, two cases were identified incidentally, supporting the well-recognized tendency of SPN to remain clinically silent until it reaches a considerable size or is detected on imaging performed for unrelated indications.

The fibrous capsule, present in 100% of our cases, is the most diagnostically reliable imaging feature of SPN. It has been identified as an independent predictor for differentiating SPN from pancreatic neuroendocrine neoplasms on both CT and MRI (10,11), typically appearing hypointense on T1- and T2-weighted sequences with moderate post-contrast enhancement, and is almost invariably present in tumors larger than 3 cm (12). The capsule arises from compressed peritumoral parenchyma and stroma, reflecting the expansile, non-infiltrative growth pattern that underlies SPN's low metastatic potential (13). Internal hemorrhage, detected in 58.3% of our cases, results from outgrowth of the central blood vessels and generates the characteristic T1-hyperintense foci on MRI. Reported rates in the literature range from 29% to 88.9%, and fluid-fluid levels may occasionally be observed (12,14,15).

The most common imaging appearance of SPN is a well-defined, encapsulated, heterogeneous mass with mixed solid-cystic morphology, reflecting variable degrees of intralesional hemorrhage and necrosis (16). This pattern was the most prevalent in our cohort (50%), consistent with published series. The solid component is typically peripheral while the cystic or necrotic component predominates centrally, although smaller lesions may present as predominantly solid masses (11,17). Two cases in our cohort demonstrated an atypical, predominantly cystic pattern with absent T1 hyperintensity, no diffusion restriction, and no internal enhancement; they were preoperatively interpreted as pseudocysts despite the absence of a history of pancreatitis or a known congenital cyst. This appearance arises when the solid component undergoes near-complete cystic degeneration and hemorrhagic products are reabsorbed (18). Atypical SPN may present across a wide imaging spectrum, ranging from purely cystic to predominantly solid lesions, and can mimic mucinous cystic neoplasms, pancreatic neuroendocrine tumors, or pseudocysts (18). Calcification, present in 18.2% of our cases and peripherally distributed in all, may provide an additional diagnostic clue (19). The presence of a preserved capsule and the clinical context of a young female patient with an encapsulated pancreatic lesion should prompt inclusion of SPN in the differential diagnosis, even in the absence of hemorrhagic signal. In equivocal cases, endoscopic ultrasound-guided fine needle aspiration may increase preoperative diagnostic yield without increasing the risk of metastasis or recurrence (20).

The reported incidence of MPD dilatation in SPN is approximately 10%, reflecting the typically soft and expansile growth pattern that displaces rather than obstructs the ductal system (21,22). In our cohort, MPD dilatation was absent in all 19 patients, irrespective of lesion size, location, or diagnosis; this included a pancreatoblastoma, which produced ductal displacement without dilatation, and an undifferentiated carcinoma, which caused biliary dilatation through common bile duct encasement without involvement of the MPD. Significant MPD dilatation should therefore prompt reconsideration of the diagnosis and raise suspicion for ductal adenocarcinoma or intraductal papillary mucinous neoplasm, both exceedingly rare in this age group (22).

Recent studies have identified several imaging features potentially associated with malignant behavior of SPN, including hepatic or peritoneal metastases, MPD obstruction, parenchymal infiltration, vascular encasement, capsular discontinuity, and tumor size exceeding 6 cm. In our series, three SPN cases exceeded 6 cm; the largest lesion measured 125 mm. None demonstrated vascular encasement, parenchymal infiltration, or nodal metastasis at surgery, underscoring the frequently indolent behavior of SPN even when size-based risk criteria are met. DWI restriction was present in 27.3% of MRI-evaluated SPN cases, likely reflecting high cellularity in solid components rather than overt malignant transformation, consistent with prior reports (23). ADC values in SPN are further influenced by cystic or hemorrhagic content, which may elevate measurements in mixed-morphology lesions and complicate threshold-based malignancy prediction (24). Detailed normative ADC data differentiating benign from malignant SPN behavior remain limited in the literature and represent an area that warrants prospective investigation.

Surgical resection is the standard of care for SPN regardless of size, given the risk of rupture and the excellent postoperative prognosis (25,26). Lymphovascular invasion was absent in all ten operated cases, and all dissected lymph nodes were reactive, consistent with the literature demonstrating that lymph node metastasis and lymphovascular spread are uncommon in SPN (27,28). PNI was identified in three of 10 patients (30%); however, its independent prognostic significance remains uncertain, as overall survival remains favorable even in the presence of adverse histopathologic features (28,29). Positive surgical margins were observed in two Whipple cases involving head-dominant lesions, reflecting the technical challenge of achieving clear margins at the superior mesenteric vein interface. Irtan et al. (30) identified positive surgical margins and age below 13.5 years as independent risk factors for recurrence, and several series have confirmed that R1 resection confers a higher recurrence risk than R0. Both margin-positive patients in our series have uninvolved posterior and lateral margins and remain under active follow-up, without evidence of recurrence.

Pancreatoblastoma is the most common malignant primary pancreatic tumor in children below 10 years, but may occur in older children and adolescents, as illustrated by our 15-year-old patient (31). Palpable abdominal mass, abdominal pain, and elevated AFP are the most frequent clinical presentations; however, AFP was

not measured preoperatively in our case, representing a limitation (31). On imaging, pancreatoblastoma typically presents as a large, well-circumscribed heterogeneous mass with solid and cystic components, internal septations, and variable calcifications; biliary duct dilatation is uncommon despite tumor size (31). In our case, IVC compression detected on USG highlights the importance of vascular interrogation in large head-uncinate lesions, as vascular encasement has direct implications for surgical planning. Nuclear beta-catenin positivity reflects shared Wnt-APC pathway activation with SPN; however, co-expression of trypsin, synaptophysin, lipase, BCL10, chromogranin, and AFP, alongside the defining squamoid nests on histology, reliably distinguishes pancreatoblastoma from SPN (32).

Among the rare entities in this series, several imaging-based diagnostic considerations merit emphasis. In the DLBCL case, the most discriminative feature was multisegmental extrapancreatic involvement, including colonic wall thickening and diffuse ascites accompanying a relatively small pancreatic body lesion. Vascular displacement without invasion and absent MPD dilatation favor lymphoma over ductal adenocarcinoma and should prompt image-guided biopsy rather than surgical exploration (33). The undifferentiated carcinoma case demonstrated vascular encasement and biliary obstruction, reflecting advanced locoregional disease. UC is an extremely rare and aggressive subtype, typically presenting as a large mass with variable imaging appearance; both biliary and pancreatic duct dilatation may occur due to the intraductal growth pattern (33). Large encasing pancreatic masses in young patients should not be reflexively attributed to lymphoma without a tissue diagnosis. In the NET G1 case, a disproportionately large imaging appearance relative to actual tumor size reflected prominent desmoplastic fibro-inflammatory stroma, a recognized pitfall that may lead to overestimation of tumor extent (34). VHL-associated pancreatic cysts develop in 60–72% of affected individuals and carry no malignant potential as isolated lesions (35). In our 17-year-old male patient, USG and MRI revealed multiple simple cysts without solid components or internal enhancement, consistent with VHL cysts without neoplastic transformation. The presence of multiple small pancreatic cysts in a young patient raises the possibility of underlying VHL disease. Surgical resection remains an option in symptomatic cases, though this is infrequent (35).

Study Limitations

This study has several limitations inherent to its retrospective single-center design. Different imaging modalities were used across patients according to clinical urgency and institutional availability, precluding a systematic cross-modality comparison. Two SPN patients refused surgery; their inclusion was based on concordant multiparametric imaging findings meeting established radiologic diagnostic criteria. Follow-up data were not uniformly available for survival analysis. Prospective multicenter studies with standardized imaging protocols and long-term follow-up are needed to validate imaging-prognostic correlations in this population.

CONCLUSION

SPN is the predominant pancreatic mass among pediatric and young adult patients and displays characteristic imaging features, including a well-defined capsule, internal hemorrhage, mixed solid-cystic morphology and absence of MPD dilatation that support a confident preoperative diagnosis in the majority of cases. An atypical, predominantly cystic SPN pattern that mimics a pseudocyst on MRI represents an underrecognized pitfall and should be considered in young female patients with an encapsulated pancreatic lesion lacking T1 hyperintensity. Each rare entity, including pancreatoblastoma, lymphoma, undifferentiated carcinoma, NET, nesidioblastosis, serous cystadenoma, and VHL-associated cysts, carries distinct imaging signatures that reflect its underlying biology and guide management; familiarity with this full diagnostic spectrum is required for appropriate clinical decision-making in this age group.

Ethics

Ethics Committee Approval: This study was conducted in accordance with the Declaration of Helsinki. Ethical approval was obtained from the Gazi University Clinical Research Ethics Committee (decision number: 10, date: 02.06.2026). The requirement for informed consent was waived by the ethics commission due to the retrospective design of the study.

Informed Consent: All patient images included in the manuscript were fully anonymized, and no identifying information is present in the figures. Patients aged 40 years or younger who presented with a pancreatic mass between 2012 and 2025 were eligible.

Footnotes

Authorship Contributions

Concept: M.Y., Design: M.Y., İ.A., Data Collection or Processing: M.Y., İ.A., Analysis or Interpretation: M.Y., İ.A., Literature Search: M.Y., Writing: M.Y.

Conflict of Interest: No conflict of interest was declared by the authors.

Financial Disclosure: The authors declared that this study received no financial support.

REFERENCES

1. Papavramidis T, Papavramidis S. Solid pseudopapillary tumors of the pancreas: review of 718 patients reported in English literature. J Am Coll Surg. 2005; 200: 965-72.
2. Yu P, Cheng X, Du Y, Yang L, Xu Z, Yin W, et al. Solid pseudopapillary neoplasms of the pancreas: a 19-year multicenter experience in China. J Gastrointest Surg. 2015; 19: 1433-40.
3. Eklund MJ, States LJ, Acord MR, Alazraki AL, Behr GG, El-Ali AM, et al. Imaging of pediatric pancreas tumors: a COG Diagnostic Imaging Committee/SPR Oncology Committee White Paper. Pediatr Blood Cancer. 2023; 70: e29975.
4. Fu C, Li X, Wang Y, Wang C, Jin H, Liu K, et al. Solid pseudopapillary neoplasm of the pancreas: a retrospective study of 195 cases. Front Oncol. 2024; 14: 1349282.
5. Shet NS, Cole BL, Iyer RS. Imaging of pediatric pancreatic neoplasms with radiologic-histopathologic correlation. AJR Am J Roentgenol. 2014; 202: 1337-48.
6. Ozcan HN, Oguz B, Sen HS, Akyuz C, Haliloglu M. Imaging features of primary malignant pancreatic tumors in children. AJR Am J Roentgenol. 2014; 203: 662-7.
7. Doi S, Yamada T, Kito Y, Obara S, Fujii Y, Nishimura T, et al. Adult-onset focal nesidioblastosis with nodular formation mimicking insulinoma. J Endocr Soc. 2022; 6: bvab185.

8. Patterson KN, Trout AT, Shenoy A, Abu-El-Haija M, Nathan JD. Solid pancreatic masses in children: a review of current evidence and clinical challenges. Front Pediatr. 2022; 10: 966943.
9. Law JK, Ahmed A, Singh VK, Akshintala VS, Olson MT, Raman SP, et al. A systematic review of solid-pseudopapillary neoplasms: are these rare lesions? Pancreas. 2014; 43: 331-7.
10. Khristenko E, Gaida MM, Tjaden C, Steinle V, Loos M, Krieger K, et al. Imaging differentiation of solid pseudopapillary neoplasms and neuroendocrine neoplasms of the pancreas. Eur J Radiol Open. 2024; 12: 100576.
11. Sunkara S, Williams T, Myers D, Kryvenko O. Solid pseudopapillary tumours of the pancreas: spectrum of imaging findings with histopathological correlation. Br J Radiol. 2012; 85: e1140-4.
12. Chae SH, Lee JM, Baek JH, Shin CI, Yoo MH, Yoon JH, et al. Magnetic resonance imaging spectrum of solid pseudopapillary neoplasm of the pancreas. J Comput Assist Tomogr. 2014; 38: 249-57.
13. Lu X, Chen H, Zhang T. Solid pseudopapillary neoplasm of the pancreas: current understanding on its malignant potential and management. Discov Oncol. 2024; 15: 77.
14. Ventriglia A, Manfredi R, Mehrabi S, Boninsegna E, Negrelli R, Pedrinolla B, et al. MRI features of solid pseudopapillary neoplasm of the pancreas. Abdom Imaging. 2014; 39: 1213-20.
15. Guerrache Y, Soyer P, Dohan A, Faraoun SA, Laurent V, Tasu JP, et al. Solid-pseudopapillary tumor of the pancreas: MR imaging findings in 21 patients. Clin Imaging. 2014; 38: 475-82.
16. Anil G, Zhang J, Al-Hamar NE, Nga ME. Solid pseudopapillary neoplasm of the pancreas: CT imaging features and radiologic-pathologic correlation. Diagn Interv Radiol. 2017; 23: 94-9.
17. Rogowska J, Semeradt J, Durko Ł, Małecka-Wojciesko E. Diagnostics and management of pancreatic cystic lesions: new techniques and guidelines. J Clin Med. 2024; 13: 4644.
18. Gao Y, Guo F, Lu Z, Xi C, Wei J, Jiang K, et al. Perioperative safety and prognosis following parenchyma-preserving surgery for solid pseudopapillary neoplasm of the pancreas. World J Surg Oncol. 2023; 21: 119.
19. Yao J, Song H. A review of clinicopathological characteristics and treatment of solid pseudopapillary tumor of the pancreas with 2450 cases in Chinese population. Biomed Res Int. 2020; 2020: 2829647.
20. Karsenti D, Caillol F, Chaput U, Perrot B, Koch S, Vuitton L, et al. Safety of endoscopic ultrasound-guided fine-needle aspiration for pancreatic solid pseudopapillary neoplasm before surgical resection: a European multicenter registry-based study on 149 patients. Pancreas. 2020; 49: 34-8.
21. Choi JY, Kim MJ, Kim JH, Kim SH, Lim JS, Oh YT, et al. Solid pseudopapillary tumor of the pancreas: typical and atypical manifestations. AJR Am J Roentgenol. 2006; 187: W178-86.
22. Kovac JD, Djikic-Rom A, Bogdanovic A, Jankovic A, Grubor N, Djuricic G, et al. The role of MRI in the diagnosis of solid pseudopapillary neoplasm of the pancreas and its mimickers: a case-based review with emphasis on differential diagnosis. Diagnostics. 2023; 13: 1074.
23. Perez ES, Towbin AJ, Morgan D, Towbin RB. Solid pseudopapillary tumor of the pancreas. Pediatr Imaging Case Ser. 2024; 20.
24. Quencer K, Kambadakone A, Sahani D, Guimaraes AS. Imaging of the pancreas: part 1. Appl Radiol. 2013; 42: 14-20.
25. Cruz MAA, Moutinho-Ribeiro P, Costa-Moreira P, Macedo G. Solid pseudopapillary neoplasm of the pancreas: unfolding an intriguing condition. GE Port J Gastroenterol. 2022; 29: 151-62.
26. Chen CC, Feng TY, Jan HC, Chou SJ, Chen TH, Wang SC. Rare case of solid pseudopapillary neoplasm of the pancreas with liver and splenic metastasis in a 19-year-old girl. Int J Surg Case Rep. 2024; 120: 109867.
27. Solakoğlu Kahraman D, Diniz G, Özamrak BG, Değirmenci M, Çalık B. Solid pseudopapillary neoplasm of the pancreas: clinicopathologic features, review of the literature. Anatol J Gen Med Res. 2025.
28. Lin YJ, Burkhart R, Lu TP, Wolfgang C, Wright M, Zheng L, et al. Solid pseudopapillary neoplasms of the pancreas across races demonstrate disparities with comparably good prognosis. World J Surg. 2022; 46: 3072-80.
29. Lee G, Sung YN, Kim SJ, Lee JH, Song KB, Hwang DW, et al. Large tumor size, lymphovascular invasion, and synchronous metastasis are associated with the recurrence of solid pseudopapillary neoplasms of the pancreas. HPB. 2021; 23: 220-30.
30. Irtan S, Galmiche-Rolland L, Elie C, Orbach D, Sauvat F, Elias D, et al. Recurrence of solid pseudopapillary neoplasms of the pancreas: results of a nationwide study of risk factors and treatment modalities. Pediatr Blood Cancer. 2016; 63: 1515-21.
31. Qiu L, Trout AT, Ayyala RS, Szabo S, Nathan JD, Geller JI, et al. Pancreatic masses in children and young adults: multimodality review with pathologic correlation. Radiographics. 2021; 41: 1766-84.
32. Omiyale AO. Adult pancreatoblastoma: current concepts in pathology. World J Gastroenterol. 2021; 27: 4172-84.
33. Veron Sanchez A, Santamaria Guinea N, Cayon Somacarrera S, Bennouna I, Pezzullo M, Bali MA. Rare solid pancreatic lesions on cross-sectional imaging. Diagnostics. 2023; 13: 2719.
34. Khanna L, Prasad SR, Sunnapwar A, Kondapaneni S, Dasyam A, Tammisetti VS, et al. Pancreatic neuroendocrine neoplasms: 2020 update on pathologic and imaging findings and classification. Radiographics. 2020; 40: 1240-62.
35. Charlesworth M, Verbeke CS, Falk GA, Walsh M, Smith AM, Morris-Stiff G. Pancreatic lesions in von Hippel-Lindau disease? A systematic review and meta-synthesis of the literature. J Gastrointest Surg. 2012; 16: 1422-1428.